**Structural Engineering and Mechanics**, *Vol. 74, No. 1 (2020) 83-90*
DOI: https://doi.org/10.12989/sem.2020.74.1.083


# Effect of material transverse distribution profile on buckling of thick functionally graded material plates according to TSDT

Wael G. Abdelrahman*

*Department of Aerospace Engineering, King Fahd University of Petroleum & Minerals, Dhahran, 31261, Saudi Arabia*

*(Received December 22, 2018, Revised October 15, 2019, Accepted November 12, 2019)*

**Abstract.** Several classical and higher order plate theories were used to study the buckling of functionally graded material (FGM) plates. In the great majority of research, a power function is used to represent metal and ceramic material transverse distribution (P-FGM). Therefore, the effect of having other transverse variation of material properties on the buckling behavior of thick rectangular FGM plates was not properly addressed. In the present work, this effect is investigated using the Third order Shear Deformable Theory (TSDT) for the case of simply supported FGM plate. Both a sigmoid function and an exponential functions are used to represent the transverse gradual property variation. The plate governing equations are combined with a Navier type expanded solution of the unknown displacements to derive the buckling equation in terms of the pre-buckling in-plane loads. Finally, the critical in-plane load is calculated for the different buckling modes. The model is verified by a comparison of the calculated buckling loads with available published results of Al-SiC P-FGM plates. The conducted parametric study shows that manufacturing FGM plates with sigmoid variation of properties in the thickness direction increases the buckling load considerably. This improvement is found to be more significant for the case of thick plates than that of thin plates. Results also show that this stiffening-like effect of the sigmoid function profile is more evident for cases where the in-plane loads are applied along the shorter edge of the plate.

**Keywords:** functionally graded materials; buckling; thick plates; simply supported; sigmoid function; P-FGM, S-FGM; E-FGM

## 1. Introduction

Functionally graded materials (FGM) were first manufactured more than thirty years ago, and are currently used in a variety of applications. The gradual variation of properties of metal/ceramic FGM plates from properties of one constituent on one face to those of the other constituent on the opposite face allows FGM plates to provide heat resistance, while maintaining good strength, fracture resistance, and low weight. Moreover, FGM plates do not suffer from the property mismatch surfaces of typical composites. As described by Thai et al. (2015), this reduces problems of residual stresses, debonding, and cracking.

Commonly used FGM plates include metal-ceramic and ceramic-ceramic plates. They can also be classified according to how the macro-scale material properties are varied during manufacturing. Analytically, this is controlled by the function describing the variation of constituent volume fraction across the thickness of the plate. Commonly used functions are the power functions (P-FGM), sigmoid functions (S-FGM), and exponential functions (E-FGM). S-FGM plates do not exhibit the rapid change of properties on one face, as in the case of P-FGM, because of the use of two functions for the definition of the volume fraction. Most of the static, dynamic, and stability analyses available in the literature are performed on P-FGM plates, as shown by the extensive review of Swaminathan et al. (2015).

Several approaches were used to study the elastic buckling problems of composite plates, including FGM plates. These included micromechanical as well as structural approaches. As examples of work based on the micromechanical approach, Bouazza *et al*. (2007) and Adda-bedia *et al*. (2008) studied the reduction in composite plate stiffness due to hygrothermal aging. More recently, this approach was also utilized to study the interfacial stresses in composite plates supported by one dimensional reinforcement (Antar *et al*. 2019). With regards to the structural approach, the governing equations obtained using classical plate theory (CPT), suitable for thin plates, were extensively solved to determine the buckling load under different types of support conditions (Javaheri and Eslami 2002, Mohammadi et al. 2010). Other research efforts focused on finding the critical temperature to cause thermal buckling of FGM plates with, and without, elastic supports (Kiani *et al*. 2011, Ghannadpour *et al*. 2012, Bouazza *et. al*. 2011a). To account for shear deformation effects in moderately thick plates, Bouazza *et al*. (2010) used Navier solution to solve the governing equations derived using first order shear deformation theory (FSDT). Other researchers utilized a finite element formulation based on the same theory to investigate buckling of simply supported FGM skew plates under in-plane mechanical loads (Ganapathi *et al*. 2006). The FSDT was later used in Hadji *et al*. (2016) in combination with the neutral surface concept to study both static and dynamic behavior of P-FGM plates. Other

*Corresponding author, Ph.D.
E-mail: wgamal@kfupm.edu.sa



ISSN: 1225-4568 (Print), 1598-6217 (Online)

variations of FSDT were used in the works of Bouazza et al. (2011b) to study thermal buckling of moderately thick P-FGM plates, and by Bourada *et al*. (2019) to obtain a novel direct formula for the Euler stability stress of moderately thick rectangular plates.

Researchers also utilized the TSDT to study buckling of thick FGM plates without the need of the FSDT problem-dependent correction factor. For example, Reddy (2000) derived an analytical formulation based on TSDT that incorporated both mechanical and thermal loads, time dependence, and geometric nonlinearity for the case of thick P-FGM plates. Later, Bdaghi and Saidi (2010) used TSDT to develop the equations of equilibrium and stability of P-FGM rectangular plates. Then, they converted the system of equations into two uncoupled equations that were solved using a Levy-type expansion. Some other types of displacement distributions, mainly trigonometric, were also explored. Benchohra *et al*. (2018) used these distributions, that satisfy the stress-free surface conditions, to arrive at a smaller number of governing equations using the Hamilton principle. These studies were not confined to the typical FGM plates. Other FGM structures that were investigated under buckling conditions included P-FGM sandwich plates, as in the work of El-Haina *et al*. (2017), where the same sinusoidal shear deformation distribution was employed.

Higher order shear deformation theories were used to study, not only mechanical buckling, but also thermal buckling behavior of FGM plates (Bouderba *et al*. 2016, Becheri *et al.* 2016) and the post-buckling response (Bakora and Tounsi 2015, Amara *et al*. 2016). Again, investigators used only the power-law distribution for the variation of material properties across the thickness of the plate. Nth-order shear deformation theories were initially used to study buckling and free vibration of laminated plates (Becheri *et al*. 2016, Bouazza *et al.* 2017, Bouazza *et al.* 2019a, Abdelmalek *et al*. 2019). The simplified versions of these theories had only two variables and resulted in transverse shear stresses satisfying the free surface condition. Other applications of the HSDT-based formulations included the investigation of buckling magnetoelectroelastic plates resting on Pasternak foundations (Ellali *et al*. 2018). In this work, the effects of mechanical, electric, magnetic loads, and use of HSDT were investigated.

More recently, researchers used hyperbolic shear deformation functions to study mechanical and thermal stability behavior of thick isotropic, composite, and FGM plates (Fellah *et al*. 2019, Bouazza *et al*. 2016a, Bouazza *et al.* 2019b). Unlike FSDT, formulations using hyperbolic shape functions do not require a correction factor. Bouazza et al. (2016b) extended this work to investigate thermal buckling of FGM nanoplates using a four-variable plate model. A two-variable refined model based on the hyperbolic shear deformation theory was used to investigate the effect of material composition on mechanical behavior of P-FGM plates (Bouazza *et al*. 2018a). The same theory was also utilized to study the mechanical behavior of layered plates under a hygrothermal environment (Bouazza and Zenkour 2018), the buckling response of P-FGM plates resting on elastic foundations (Soltani et al. 2019), and the thermal buckling of FGM nanoplates (Bouazza *et al*. 2016, Bouazza *et al*. 2018b).

With the continuous advancement in computational mechanics, isogeometric analysis (IGA) emerged as a powerful tool in studying the behavior of FGM plates, among other things. Valizadeh et al. (2013) used a non-uniform rational B-spline (NURBS) based isogeometric finite element method to study both linear static and dynamic behaviors of FGM plates. The element, which utilized FSDT still required the evaluation of correction factors, and included a modification to alleviate shear locking. Based on NURBS and Reissner-Mindlin plate theory, Yin *et al*. (2016) extracted the critical buckling parameters and natural frequencies of defective FGM plates. Later, Yin *et al*. (2017) used high order continuity splines basis functions to develop Kirchhoff-Love element that proved to be more effective than C1 conforming finite element approximations. Researchers also used an extended isogeometric analysis (XIGA) that is capable of capturing discontinuities of internal defects. Associating this analysis with either the simple first-order shear deformation theory (S-FSDT) or the simple quasi-3D hyperbolic shear deformation theory (S-Q3HSDT), they investigated thermal buckling of plates with, and without, internal voids (Yin *et al*. 2014, Yu *et al*. 2016, Liu *et al.* 2017, Yu *et al.* 2017). Using these formulations, with a fewer number of displacement distribution variables, proved to be computationally efficient. A variant of the theory, called the refined plate theory (RPT), with only four displacement variables was used to investigate thermal buckling of simply supported P-FGM plates under different types of loading conditions. (Bouazza and Benseddiq 2015).

There has been always considerable interest to develop even new refined higher order shear deformation theories. In some of these theories, the specific displacement field distribution was not assumed a priori, but was obtained from the theory of elasticity. For example, a finite element formulation was associated with S-TSDT that has kinematics derived from the theory of elasticity (Bui *et al*. 2016). This model was utilized to study the mechanical behavior of P-FGM plates under the effect of high temperatures. Yin *et al*. (2016) combined IGA with a similar refined theory to study the effects of the in-plane material inhomogeneity on the buckling of P-FGM plates. With the use NURBS, both exact geometric representationgh order approximation were achieved. Finally, Vu *et al*. (2018) extended the work by using a refined simple third-order shear deformation theory (R-STSDT), with shape functions built by the Kriging technique. This simplified the process of enforcing the essential boundary conditions. The formulation was used to investigate the bending, buckling, and free vibration of P-FGM plates.

Therefore, it is clear from literature review that regardless of the order of the shear deformation theory that was used, the formulations focused on applications to P-FGM plates. The effect of having a different through-thickness mechanical properties' distribution function on the buckling response of thick FGM plates has not been adequately studied yet. The major contribution in the present work is the investigation of this effect, by

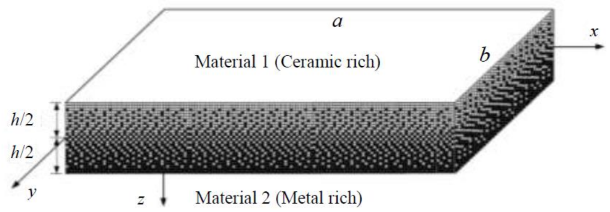


Fig. 1 Geometry and coordinate system of metal-ceramic FGM plate

considering the sigmoid and exponential functions, in addition to the commonly used power law function. In order to achieve this, a TSDT formulation is solved using a Navier-type expansion, and is used to calculate the buckling critical load for the cases of uniaxial and biaxial loading.

## 2. Methodology

Several deformation models are used for the construction of the buckling problem of FGM plates. These include the CPT, FSDT, and several formulations of HSDT. In this work, the TSDT, which is suitable for describing moderately-thick to thick plates, is employed. With regards to material properties, the FGM plate is assumed to have temperature-independent properties, that vary only along the thickness direction. The spatial distribution of material properties, including the elastic modulus and Poisson's ratio, is dependent on this variation.

Consider the rectangular thick metal-ceramic FGM plate shown in Fig. 1. The variation of material properties along the z-direction, from that of the metal rich upper surface to the ceramic rich lower surface, depends on the through-thickness distribution of volume fraction of both constituents. For the commonly used power law distribution, this gives the following expression for Young's modulus in P-FGM plates:

$$E(z) = \left(\frac{h/2+z}{h}\right)^p E_1 + \left[1 - \left(\frac{h/2+z}{h}\right)^p\right] E_2 \tag{1}$$

where $p$ is the power-law parameter, $E_1$ and $E_2$ are Young's moduli of the ceramic and metal materials; respectively. The rapid change of properties associated with this distribution at the plate face can be reduced if two power law functions are used to represent the volume fraction variation, resulting in the S-FGM property distribution:

$$E(z) = \begin{cases} E_2 - \dfrac{1}{2}\left(\dfrac{\frac{h}{2}+z}{\frac{h}{2}}\right)^p (E_2 - E_1) & -\dfrac{h}{2} \le z \le 0 \\ E_1 - \dfrac{1}{2}\left(\dfrac{\frac{h}{2}-z}{\frac{h}{2}}\right)^p (E_1 - E_2) & 0 \le z \le \dfrac{h}{2} \end{cases} \tag{2}$$

When an exponential function is used for the volume fraction distribution, then Young's modulus of the E-FGM takes the form:

$$E(z) = E_2 e^{\left(\frac{h/2+z}{h}\right) ln\,(\frac{E_1}{E_2})} \tag{3}$$

The variation of the material Poisson's ratio follows expressions similar to Eqs. (1)-(3). The displacement field of the TSDT, in terms of the displacements and rotations of the transverse normal to the mid-plane, is given by Reddy (2000):

$$u(x,y,z) = u_0(x,y) + z\phi_x(x,y) - cz^3(\phi_x + \frac{\partial w}{\partial x}) \tag{4}$$

$$v(x,y,z) = v_0(x,y) + z\phi_y(x,y) - cz^3(\phi_y + \frac{\partial w}{\partial y}) \tag{5}$$

$$w(x,y,z) = w_0(x,y) \tag{6}$$

where the 0 denotes a midplane value of displacement, and where $\phi_x$, $\phi_y$ are the rotations of the transverse normal to the midplane. This field results in the five total strain components, given by:

$$\begin{Bmatrix} \varepsilon_{xx} \\ \varepsilon_{yy} \\ \gamma_{xy} \end{Bmatrix} = \begin{Bmatrix} \dfrac{\partial u_0}{\partial x} \\ \dfrac{\partial u_0}{\partial y} \\ \dfrac{\partial u_0}{\partial y} + \dfrac{\partial v_0}{\partial x} \end{Bmatrix} + z \begin{Bmatrix} \dfrac{\partial \phi_x}{\partial x} \\ \dfrac{\partial \phi_y}{\partial y} \\ \dfrac{\partial \phi_x}{\partial y} + \dfrac{\partial \phi_y}{\partial x} \end{Bmatrix} - c\, z^3 \begin{Bmatrix} \dfrac{\partial \phi_x}{\partial x} + \dfrac{\partial^2 w_0}{\partial x^2} \\ \dfrac{\partial \phi_y}{\partial y} + \dfrac{\partial^2 w_0}{\partial y^2} \\ \dfrac{\partial \phi_x}{\partial y} + \dfrac{\partial \phi_y}{\partial x} + 2\dfrac{\partial^2 w_0}{\partial x \partial y} \end{Bmatrix}, \tag{7}$$

$$\begin{Bmatrix} \gamma_{yz} \\ \gamma_{xz} \end{Bmatrix} = \begin{Bmatrix} \phi_y + \dfrac{\partial w_0}{\partial y} \\ \phi_x + \dfrac{\partial w_0}{\partial x} \end{Bmatrix} - 3c\, z^2 \begin{Bmatrix} \phi_y + \dfrac{\partial w_0}{\partial y} \\ \phi_x + \dfrac{\partial w_0}{\partial x} \end{Bmatrix}$$

Using one of the through-thickness distribution of material properties, Eqs. (1), (2), or (3), the constitutive relations describing the stresses in terms of the mechanical strain component take the form:

$$\begin{Bmatrix} \sigma_{xx} \\ \sigma_{yy} \\ \sigma_{zz} \\ \sigma_{xz} \\ \sigma_{xy} \end{Bmatrix} = \begin{bmatrix} Q_{11} & Q_{12} & 0 & 0 & 0 \\ Q_{12} & Q_{11} & 0 & 0 & 0 \\ 0 & 0 & Q_{44} & 0 & 0 \\ 0 & 0 & 0 & Q_{55} & 0 \\ 0 & 0 & 0 & 0 & Q_{66} \end{bmatrix} \begin{Bmatrix} \hat{\varepsilon}_{xx} \\ \hat{\varepsilon}_{yy} \\ \gamma_{yz} \\ \gamma_{xz} \\ \gamma_{xy} \end{Bmatrix} \tag{8}$$

where the elastic coefficients $Q_{ij}$ are:

$$Q_{11} = \frac{E(z)}{1-\nu^2}, \quad Q_{12} = \nu Q_{11}, \quad Q_{44} = Q_{55} = Q_{66} = \frac{E(z)}{2(1+\nu)} \tag{9}$$

The inplane force resultants and moment resultants can be defined as:

$$\begin{Bmatrix} N_{xx} \\ N_{yy} \\ N_{xy} \end{Bmatrix} = \int_{-h/2}^{h/2} \begin{Bmatrix} \sigma_{xx} \\ \sigma_{yy} \\ \sigma_{xy} \end{Bmatrix} dz \ , \ \begin{Bmatrix} M_{xx} \\ M_{yy} \\ M_{xy} \end{Bmatrix} = \int_{-h/2}^{h/2} \begin{Bmatrix} \sigma_{xx} \\ \sigma_{yy} \\ \sigma_{xy} \end{Bmatrix} zdz \qquad (10)$$

whereas the higher-order resultants are defined in a similar manner using higher powers of $z$. The equilibrium equations of the plate can then be written as::

$$\frac{\partial N_{xx}}{\partial x} + \frac{\partial N_{xy}}{\partial y} = 0 \qquad (11.a)$$

$$\frac{\partial N_{xy}}{\partial x} + \frac{\partial N_{yy}}{\partial y} = 0 \qquad (11.b)$$

$$\frac{\partial \bar{Q}_x}{\partial x} + \frac{\partial \bar{Q}_y}{\partial y} + c_1 \left( \frac{\partial^2 P_{xx}}{\partial x^2} + 2\frac{\partial^2 P_{xy}}{\partial x \partial y} + \frac{\partial^2 P_{yy}}{\partial y^2} \right) + q = 0 \qquad (11.c)$$

$$\frac{\partial \bar{M}_{xx}}{\partial x} + \frac{\partial \bar{M}_{xy}}{\partial y} - \bar{Q}_x = 0 \qquad (11.d)$$

$$\frac{\partial \bar{M}_{xy}}{\partial x} + \frac{\partial \bar{M}_{yy}}{\partial y} - \bar{Q}_y = 0 \qquad (11.e)$$

where

$$q = N_x \frac{\partial^2 w}{\partial x^2} + 2N_{xy} \frac{\partial^2 w}{\partial x \partial y} + N_y \frac{\partial^2 w}{\partial y^2}$$

Eqs. (11.a)-(11.e) can be solved using any of the strong solutions, including Navier–type solution, for the case of four plate simply-supported boundaries. This solution satisfies all the boundary conditions using the displacement expansions:

$$u_0(x,y,t) = \sum_{n=1}^{\infty} \sum_{m=1}^{\infty} U_{mn}(t) \cos(a_f x) \sin(b_f y) \qquad (12.a)$$

$$v_0(x,y,t) = \sum_{n=1}^{\infty} \sum_{m=1}^{\infty} V_{mn}(t) \sin(a_f x) \cos(b_f y) \qquad (12.b)$$

$$w_0(x,y,t) = \sum_{n=1}^{\infty} \sum_{m=1}^{\infty} W_{mn}(t) \sin(a_f x) \sin(b_f y) \qquad (12.c)$$

$$\phi_x(x,y,t) = \sum_{n=1}^{\infty} \sum_{m=1}^{\infty} X_{mn}(t) \cos(a_f x) \sin(b_f y) \qquad (12.d)$$

$$\phi_y(x,y,t) = \sum_{n=1}^{\infty} \sum_{m=1}^{\infty} Y_{mn}(t) \sin(a_f x) \cos(b_f y) \qquad (12.e)$$

Substituting the series expansions Eq. (12) into the equations of motions, the plate buckling equation becomes:

$$\begin{bmatrix} s_{11} & s_{12} & s_{13} & s_{14} & s_{15} \\ s_{12} & s_{22} & s_{23} & s_{24} & s_{25} \\ s_{13} & s_{23} & s_{33}+k & s_{34} & s_{35} \\ s_{14} & s_{24} & s_{34} & s_{44} & s_{45} \\ s_{15} & s_{25} & s_{35} & s_{45} & s_{55} \end{bmatrix} \begin{Bmatrix} U_{mn} \\ V_{mn} \\ W_{mn} \\ X_{mn} \\ Y_{mn} \end{Bmatrix} = \underline{0} \qquad (13)$$

where the plate stiffness matrix elements $s_{ij}$ are expressed as in Reddy (2000):

$$\begin{aligned} s_{11} &= A_{11}a_f^2 + A_{66}b_f^2, \\ s_{12} &= (A_{12} + A_{66})a_f b_f, \\ s_{13} &= -c_1\left[E_{11}a_f^2 + (E_{12} + 2E_{66})b_f^2\right]a_f, \\ s_{14} &= \hat{B}_{11}a_f^2 + \hat{B}_{66}b_f^2, \\ s_{15} &= \left(\hat{B}_{12} + \hat{B}_{66}\right)a_f b_f, \\ s_{22} &= A_{66}a_f^2 + A_{22}b_f^2, \\ s_{23} &= -c_1\left[E_{22}b_f^2 + (E_{12} + 2E_{66})a_f^2\right]b_f, \\ s_{24} &= \hat{s}_{15}, \\ s_{25} &= \hat{B}_{66}a_f^2 + \hat{B}_{22}b_f^2, \\ s_{33} &= \bar{A}_{55}a_f^2 + \bar{A}_{44}b_f^2 + c_1[H_{11}a_f^4 + 2(H_{12} + 2H_{66})a_f^2 b_f^2 + H_{22}b_f^4 \ , \\ s_{34} &= \bar{A}_{55}a_f - c_1\left[\hat{F}_{11}a_f^3 + \left(\hat{F}_{12} + 2\hat{F}_{66}\right)a_f b_f^2\right], \\ s_{35} &= \bar{A}_{44}b_f - c_1\left[\hat{F}_{22}b_f^3 + \left(\hat{F}_{12} + 2\hat{F}_{66}\right)a_f^2 b_f\right], \\ s_{44} &= \bar{A}_{55} + \bar{D}_{11}a_f^2 + \bar{D}_{66}b_f^2, \\ s_{45} &= (\bar{D}_{12} + \bar{D}_{66})a_f b_f, \\ s_{55} &= \bar{A}_{44} + \bar{D}_{66}a_f^2 + \bar{D}_{22}b_f^2 \end{aligned} \qquad (14)$$

In Eq. (13):

$$k = N_{cr}\left(\gamma_1 {a_f}^2 + \gamma_2 {b_f}^2\right) \qquad (15)$$

where $a_f = m\pi/a$ and $b_f = n\pi/b$.

In Eqs. (14), the stiffness elements are calculated from the two reduced matrices $\bar{A}_{ij}$, $\bar{D}_{ij}$, given by:

$$\begin{aligned} \bar{A}_{ij} &= A_{ij} - 2c_1 D_{ij} + c_1^2 F_{ij} \qquad (i.j = 1,2,3) \\ \bar{D}_{ij} &= D_{ij} - 2c_1 F_{ij} + c_1^2 H_{ij} \qquad (i.j = 1,2,3) \\ \bar{A}_{ij} &= A_{ij} - 6c_1 D_{ij} + 9c_1^2 F_{ij} \qquad (i.j = 4,5) \end{aligned} \qquad (16)$$

And where the matrices with the ^ sign are developed only for expression simplification purposes, and are given by (Reddy 2000):

$$\begin{aligned} \hat{A}_{ij} &= A_{ij} - c_1 D_{ij}, \ \hat{B}_{ij} = B_{ij} - c_1 E_{ij}, \ (i.j = 1,2,3) \\ \hat{D}_{ij} &= D_{ij} - c_1 F_{ij}, \ \hat{F}_{ij} = F_{ij} - c_1 H_{ij}, \ (i.j = 1,2,3) \end{aligned} \qquad (17)$$

Here, $A$, $B$, $D$, $E$, $F$, and $H$ are the commonly used equivalent plate stiffness matrices, obtained by $z$-weighted integration of $Q$ over the plate thickness. In many cases, the in-plane pre-buckling loads are defined as:

$$N_x = \gamma_1 N_{cr}, \qquad N_y = \gamma_2 N_{cr}, \qquad N_{xy} = 0 \qquad (18)$$

For nontrivial solution, the determinant of the coefficient matrix in Eq. (13) must be zero.

It is clear from the above formulation that the volume fraction and material properties' distribution function (power, sigmoid, or exponential) will affect the plate stiffness, and hence the buckling load.

## 3. Numerical Results

The suggested model is validated by comparisons with the published results of thick FGM plate buckling. Since most published work utilized the power law material properties distribution, with simply supported boundary conditions, buckling of a simply supported Al-SiC P-FGM plate is considered here for validation purposes only. Analysis of other types of FGM plates is considered afterwards. The plate thickness ratio range is taken to cover thick to moderately thick plates. The ceramic and metal constituents have the following properties: $E_1$ = 420 GPa, $E_2$ = 70 GPa = 0.3.

Table 1 shows a comparison between the predicted buckling load and the results reported by Bodaghi and Saidi (2010) for different values of plate aspect ratio ($a/b$)and thickness ratio ($b/h$). Buckling occurs in the first mode, $m = 1,\ n = 1$, except for the underlined values, where it occurs in the second mode, $m = 2,\ n = 1$. The comparison shows excellent agreement of the calculated values of buckling load with the previously reported values under various in-plane loading conditions, for the whole range of the considered variables.

Table 1 Comparison between the calculated critical buckling load of a rectangular P-FGM plate under uniaxial and biaxial in-plane loading, and the TSDT results of Bodaghi and Saidi (2010)

| $\gamma_1$, $\gamma_2$ | Aspect ratio | Thickness ratio | Model | P = 0 | 1 | 2 |
|---|---|---|---|---|---|---|
| -1, 0 | 0.5 | 10 | TSDT | 2079.72 | 1028.41 | 780.10 |
| | | | Current | 2079.76 | 1028.45 | 780.23 |
| | | 5 | TSDT | 12162.119 | 6270.298 | 4692.542 |
| | | | Current | 12164.99 | 6272.43 | 4695.03 |
| | 1 | 10 | TSDT | 1437.361 | 702.304 | 534.441 |
| | | | Current | 1437.39 | 702.25 | 534.84 |
| | | 5 | TSDT | 9915.620 | 4955.431 | 3746.054 |
| | | | Current | 9916.20 | 4955.48 | 3746.73 |
| | 1.5 | 10 | TSDT | <u>1527.903</u> | <u>748.920</u> | <u>569.751</u> |
| | | | Current | <u>1528.00</u> | <u>748.99</u> | <u>569.83</u> |
| | | 5 | TSDT | <u>10044.721</u> | <u>5067.219</u> | <u>3819.109</u> |
| | | | Current | <u>10044.96</u> | <u>5068.08</u> | <u>3820.08</u> |
| -1,-1 | 0.5 | 10 | TSDT | 1663.777 | 822.738 | 624.158 |
| | | | Current | 1663.81 | 822.76 | 624.18 |
| | | 5 | TSDT | 9729.999 | 5016.384 | 3754.274 |
| | | | Current | 9732.00 | 5017.94 | 3756.02 |
| | 1 | 10 | TSDT | 718.692 | 351.124 | 267.416 |
| | | | Current | 718.70 | 351.126 | 267.418 |
| | | 5 | TSDT | 4957.888 | 2477.589 | 1873.190 |
| | | | Current | 4958.10 | 2477.74 | 1873.37 |
| | 1.5 | 10 | TSDT | 526.861 | 256.776 | 195.714 |
| | | | Current | 526.86 | 256.78 | 195.71 |
| | | 5 | TSDT | 3772.877 | 1871.038 | 1418.120 |
| | | | Current | 3772.97 | 1871.10 | 1418.19 |

Table 2 Comparison between the buckling load values of P-, S-, and E-FGM simply supported rectangular plates with aspect ratio $a/b$=0.5 subjected to a uniaxial in-plane loading $\gamma_1$ = -1, $\gamma_2$ = 0

| $b/h$ | Type | P = 0 | 1 | 2 | 5 |
|---|---|---|---|---|---|
| 10 | P-FGM | 2079.76 | 1028.45 | 780.228 | 623.169 |
| | S-FGM | 1213.19 | 1028.45 | 922.045 | 829.984 |
| | E-FGM | 839.898 | 839.898 | 839.898 | 839.898 |
| 5 | P-FGM | 12165.0 | 6272.43 | 4695.03 | 3466.05 |
| | S-FGM | 7096.24 | 6272.43 | 5780.32 | 5342.20 |
| | E-FGM | 5032.32 | 5032.32 | 5032.32 | 5032.32 |

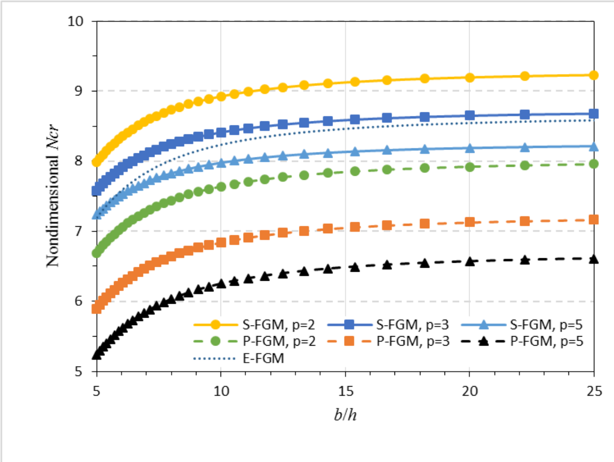


Fig. 2 Comparison between variation of the calculated nondimensional buckling load with plate thickness for square S-, P-, and E-FGM SSSS plates at different values of power $p$

Next, the effect of material property distribution function is investigated. The Al-SiC FGM plate buckling problem is considered for the cases of a plate produced with sigmoid through-thickness property variation (S-FGM), and with two parameter exponential property variation (E-FGM). Table 2 depicts the buckling load results for these two types of FGM plates, as compared to the results of P-FGM plate under uniaxial loading. Results are calculated for the cases of moderately thick, and thick plates, with $b/h$=10 and 5; respectively. The table shows that for, values of $p$ >1, S-FGM plates have higher buckling load than similar P-FGM plates. E-FGM plates have stiffness that is between P-FGM plates and S-FGM plates for values of $p$>1. This range of $p$ is of particular practical interest because it provides lower rate of change of the material properties near the ceramic face.

Fig. 2 further illustrates this behavior by depicting the variation of nondimensionalized critical buckling load $\bar{N}_{cr} = N_{cr}a^2/E_2h^3$ of a square plate with the three types of property distribution, sigmoid, power law, and exponential, at different values of $p$. The figure confirms that the stiffening effect that is exhibited by S-FGM plates over the more commonly used P-FGM plates covers all the range of plate thickness from thin to thick plates at all values of $p$>1.

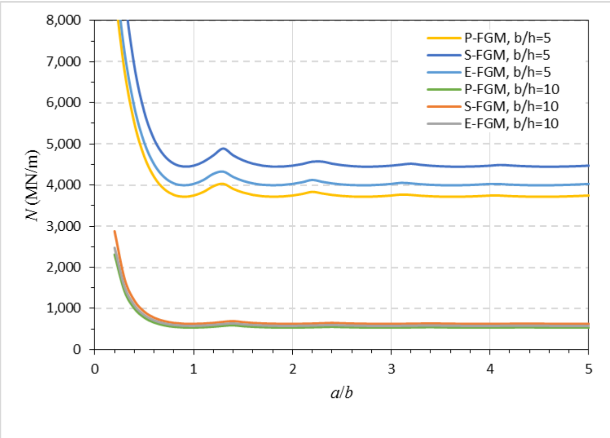


Fig. 3 Variation of the calculated buckling load with $a/b$ for Al/Sic SSSS plate under uniaxial in-plane loading, and having different property through-thickness profiles

The results of E-FGM plates are shown on the figure for comparison purposes.

Fig. 3 shows the variation of the buckling load with the side length ratio $a/b$ for the P-, S- and E-FGM simply supported plates, for the case $p$=2, under the effect of a uniaxial in-plane load in the x-direction. The figure depicts results for both moderately thick plates ($b/h$=5), and thick plates ($b/h$=5). From this figure, it is clear that the lower rate of change of material property in the S-FGM, compared to the P-FGM plates, results in a higher buckling load. It also shows that the effect of material property distribution function is more significant for the case of thick plates.

Fig. 4 depicts the percentage increase of buckling load of S-FGM plate over the P-FGM plate for the two cases of plate thickness ratio. It is evident from the figure that the extra buckling stiffness in the S-FGM decreases as the plate aspect ratio increases and the unsupported length of the plate becomes the determining factor for the instability.

In order to investigate if the drawn conclusions, regarding the higher buckling load carrying capacity of S-FGM and E-FGM over P-FGM plates, are load-type-dependent, we consider next the case of biaxial loading of the same SSSS FGM plates. Fig. 5 depicts the variation of the buckling load with the side length ratio $a/b$ for that loading condition, and for the same range of $0.2< a/b <5$, and $p$=2. Both thick and moderately thick plates are considered. The curves show the typical variation of critical biaxial buckling load with the unsupported plate length. The figure confirms the higher buckling load of S-FGM plates. It also confirms the conclusion of the uniaxial case that this extra stiffening due to type of property profile is dependent on the plate thickness ratio. Over the range of plate side ratio, that increase in buckling load drops from 32.3 % to 18 % for the thick plate case, and from only 24.5% to 16.4% for the moderately thick plate case.

## 4. Conclusions

In this study, the author utilizes a TSDT in order to arrive at the governing equations of instability of thick

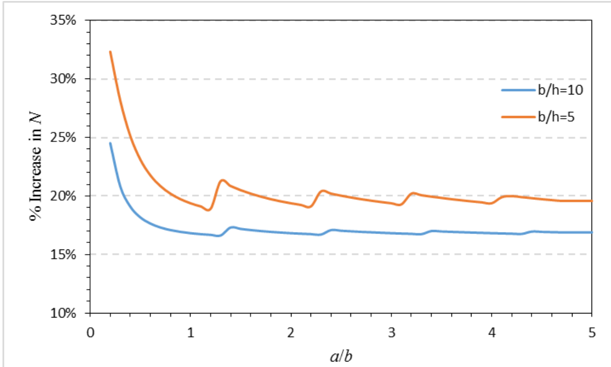


Fig. 4 Variation of the percentage increase in buckling load of SSSS S-FGM with $a/b$ =0.5 over that of a similar P-FGM plate

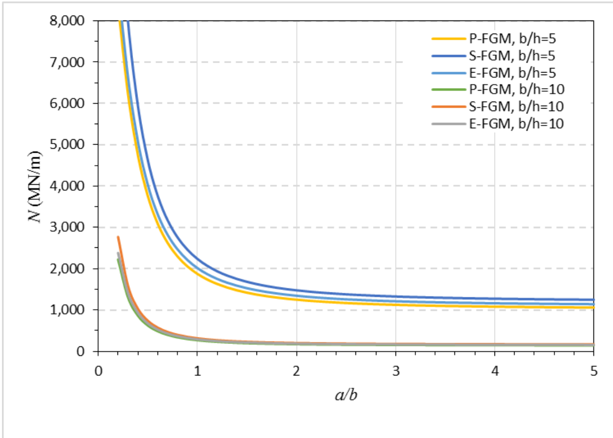


Fig. 5 Variation of the calculated buckling load with $a/b$ for Al/Sic SSSS plate under biaxial in-plane loading, and having different property through-thickness profiles

simply supported S-, P-, and E-FGM plates. A strong expansion solution that satisfies all boundary conditions is then employed to solve the governing equations. Upon verification of the modeling, S-FGM plate buckling results are compared to those of the P-FGM and E-FGM plates for several cases covering a range of plate aspect ratio and thickness ratio. Both uniaxial and biaxial in-plane loading cases are considered. The numerical study shows that plates with sigmoid function profile for the transverse variation of constituent properties have higher buckling loads than plates with power law or exponential profiles, for all values of power index $p$>1. Additionally, the results show that this effect is more significant in thick FGM plates than in thin or moderately thick plates. For the case of biaxial compression, results show that in all three considered types of FGM plates, buckling occurs in the first mode over the considered ranges of aspect ratio and thickness ratio. Finally, this increase of buckling resistance in S-FGM plates over its value in other types of FGM plates is more evident when the in-plane load is in the direction of the shorter plate side. If the applied load is along the longer dimension, then plate length has more effect, and there is only a slight increase in plate stiffness due to property transverse distribution profile. Further studies can confirm if the behavior is maintained in post-buckling or nonlinear response of the functionally graded plate.

## References


Abdelmalek, A., Bouazza, M. Zidour, M. and Benseddiq, N. (2019), "Hygrothermal effects on the free vibration behavior of composite plate using nth-order shear deformation theory: a micromechanical approach", *Iran J. Sci. Tech. Trans. Mech. Eng.*, **43**(1), 61-73. https://doi.org/10.1007/s40997-017-0140-y.

Adda-bedia, E.A., Bouazza, M., Tounsi, A., Benzair, A. and Maachouc, M. (2008), "Prediction of stiffness degradation in hygrothermal aged [$\theta_m$/$90_n$]s composite laminates with transverse cracking", *J. Mat. Process. Tech.*, **199**(1-3), 199-205. https://doi.org/10.1016/j.jmatprotec.2007.08.002.

Amara, K. Bouazza, M. and Fouad, B. (2016), "Postbuckling Analysis of Functionally Graded Beams Using Nonlinear Model", *Per. Polytech. Mech. Eng.*, **60**(2), 121-128. https://doi.org/10.3311/ppme.8854.

Antar, K., Amara, K., Benyoucef, S., Bouazza, M. and Ellali, M. (2019), "Hygrothermal effects on the behavior of reinforced-concrete beams strengthened by bonded composite laminate plates", *Str. Eng. Mech.*, **69**(3), 327-334. https://doi.org/10.14359/551.

Bakora, A. and Tounsi, A. (2015), "Thermo-mechanical post-buckling behavior of thick functionally graded plates resting on elastic foundation", *Str. Eng. Mech.*, **56** (1), 85-106. https://doi.org/10.12989/sem.2015.56.1.085.

Becheri, T., Amara, K., Bouazza, M. and Benseddiq, N. (2016), "Buckling of symmetrically laminated plates using nth-order shear deformation theory with curvature effects", *Steel Comp. Str.*, **21**(6), 1347-1368. https://doi.org/10.12989/scs.2016.21.6.1347.

Benchohra, M., Driz, H., Bakora, A., Tounsi, A., Bedia, E.A. and Hassan, S. (2018), "A new quasi-3D sinusoidal shear deformation theory for functionally graded plates", *Str. Eng. Mech.*, **65**(1), 19-31. https://doi.org/10.12989/sem.2018.65.1.019.

Bodaghi, M. and Saidi, A.R. (2010), "Levy-type solution for buckling analysis of thick functionally graded rectangular plates based on the higher-order shear deformation plate theory", *Appl. Math. Mod.*, **34**, 3659–3673. https://doi.org/10.1016/j.apm.2010.03.016.

Bouazza, M. and Benseddiq, N. (2015), "Analytical modeling for the thermoelastic buckling behavior of functionally graded rectangular plates using hyperbolic shear deformation theory under thermal loadings", *Multidisc. Mod. Mat. Struc.*, **11**(4), 558-578. https://doi.org/10.1108/mmms-02-2015-0008.

Bouazza, M. and Zenkour, A. (2018), "Free vibration characteristics of multilayered composite plates in a hygrothermal environment via the refined hyperbolic theory", *Eur. Phys. J. Plus*, **133**: 217. https://doi.org/10.1140/epjp/i2018-12050-x.

Bouazza, M., Antar, K., Amara, K., Benyoucef, S. and Bedia, E. (2019), "Influence of temperature on the beams behavior strengthened by bonded composite plates", *Geomech. Eng.*, **18**(5), 555-566. https://doi.org/10.1016/j.compstruct.2013.01.021.

Bouazza, M., Becheri, T. Boucheta, A. and Benseddiq, N. (2016), "Thermal buckling analysis of nanoplates based on nonlocal elasticity theory with four-unknown shear deformation theory resting on Winkler–Pasternak elastic foundation", *Int. J. Comp. Meth. Eng. Sci. Mech.*, **17**, 362-373. https://doi.org/10.1080/15502287.2016.1231239.

Bouazza, M., Benseddiq, N. and Zenkour, A. (2019), "Thermal buckling analysis of laminated composite beams using hyperbolic refined shear deformation theory" *J. of Therm. Str.,* **42**(3), 332-340. https://doi.org/10.1080/01495739.2018.1461042.

Bouazza, M., Kenouza, Y., Benseddiq, N. and Zenkour, A. (2017), "A two-variable simplified nth-higher-order theory for free vibration behavior of laminated plates", *Compos. Str.*, **182**, 533-541. https://doi.org/10.1016/j.compstruct.2017.09.041.

Bouazza, M., Lairedj, A., Benseddiq, N. and Khalkia, S. (2016), "A refined hyperbolic shear deformation theory for thermal buckling analysis of cross-ply laminated plates", *Mech. Res. Comm.*, **73**, 117-126. https://doi.org/10.1016/j.mechrescom.2016.02.015.

Bouazza, M., Tounsi, A., Adda-Bedia E.A. and Megueni, A. (2011), "Stability analysis of functionally graded plates subject to thermal loads", *Shell-like Struc.-Adv. Struc. Mat.*, **15**, 669-680. https://doi.org/10.1007/978-3-642-21855-2_44.

Bouazza, M., Tounsi, A., Adda-Bedia, E.A. and Megueni, A. (2010), "Thermoelastic stability analysis of functionally graded plates: An analytical approach", *Comput. Mat. Sci.*, **49**(4), 865–870. https://doi.org/10.1016/j.commatsci.2010.06.038.

Bouazza, M., Tounsi, A., Adda-Bedia, E.A. and Megueni, A. (2011), "Thermal buckling of simply supported FGM square plates", *Appl. Mech. Mat.*, **61**, 25-32. https://doi.org/10.4028/www.scientific.net/amm.61.25.

Bouazza, M., Tounsi, A., Benzair, A. and Adda-bedia, E.A. (2007), "Effect of transverse cracking on stiffness reduction of hygrothermal aged cross-ply laminates", *J. Mat. Des.*, **28**(4), 1116-1123. https://doi.org/10.1016/j.matdes.2006.02.003.

Bouazza, M., Zenkour, A. and Benseddiq, N. (2018), "Closed-from solutions for thermal buckling analyses of advanced nanoplates according to a hyperbolic four-variable refined theory with small-scale effects", *Acta Mech.,* **229**(5), 2251-2265. https://doi.org/10.1007/s00707-017-2097-8.

Bouazza, M., Zenkour, A. and Benseddiq, N. (2018), "Effect of material composition on bending analysis of FG plates via a two-variable refined hyperbolic theory", *Arch. Mech.*, **70** (2), 107-129.

Bouderba, B., Houari, M., Tounsi, A. and Mahmoud S.R. (2016), "Thermal stability of functionally graded sandwich plates using a simple shear deformation theory", *Str. Eng. Mech.*, **58**(3), 397-422. https://doi.org/10.12989/sem.2016.58.3.397.

Bourada, M., Bouadi, A., Bousahla, A., Senouci, A, Bourada, F., Tounsi, A. and Mahmoud, S. (2019), "Buckling behavior of rectangular plates under uniaxial and biaxial compression", *Str. Eng. Mech.*, **70**(1), 113-123. https://doi.org/10.12989/sem.2019.70.1.113.

Bui, T., Van Do, T., Ton, L., Doan, D., Tanaka, S., Pham, D., Nguyen-Van, T., Yu, T. and Hirose, S. (2016), "On the high temperature mechanical behaviors analysis of heated functionally graded plates using FEM and a new third-order shear deformation plate theory", *Comp. Part B: Eng.* , **92**, 218-241. https://doi.org/10.1016/j.compositesb.2016.02.048.

El-Haina, F., Bakora, A., Bousahla, A., Tounsi, A. and Mahmoud, S.R. (2017), "A simple analytical approach for thermal buckling of thick functionally graded sandwich plates," *Str. Eng. Mech.*, **63**(5), 585-595. https://doi.org/10.12989/sem.2017.63.5.585.

Ellali, M., Amara, K., Bouazza, M. and Bourada, F. (2018), "The buckling of piezoelectric plates on pasternak elastic foundation using higher-order shear deformation plate theories" *Smart Struc. Sys.*, **21**(1), 113-122. https://doi.org/10.12989/scs.2016.21.6.1347.

Fellah, M., Draiche, K., Houari, M., Tounsi, A., Saeed, T., Alhodaly, M. and Benguediab, M. (2019), "A novel refined shear deformation theory for the buckling analysis of thick isotropic plates", *Str. Eng. Mech.*, **69**(3), 335-345. https://doi.org/10.12989/sem.2019.69.3.335.

Ganapathi, M., Prakash, T. and Sundararajan, N. (2006), "Influence of functionally graded material on buckling of skew plates under mechanical loads", *J. Eng. Mech*., **132**(8), 902–905. https://doi.org/10.1061/(asce)0733-9399(2006)132:8(902).

Ghannadpour, S.A.M., Ovesy, H.R. and Nassirnia, M. (2012), "Buckling analysis of functionally graded plates under thermal loadings using the finite strip method", *Comput. Struct.*,**108**, 93–99. https://doi.org/10.1016/j.compstruc.2012.02.011.

Hadji, L., Meziane, M., Abdelhak, Z. and Hassaine, T. (2016), "Static and dynamic behavior of FGM plate using a new first shear deformation plate theory", *Str. Eng. & Mech*., **57**(1), 127-140. https://doi.org/10.12989/sem.2016.57.1.127.

Javaheri, R. and Eslami, M.R. (2002), "Buckling of functionally graded plates under in-plane compressive loading", *ZAMM J. Appl. Math. Mech.*, **82**(4), 277–283. https://doi.org/10.1002/1521-4001(200204)82:4%3C277::aid-zamm277%3E3.0.co;2-y.

Kiani, Y., Bagherizadeh, E. and Eslami, M.R. (2011), "Thermal buckling of clamped thin rectangular FGM plates resting on Pasternak elastic foundation", *ZAMM – J. Appl. Math. Mech. / Z Angew. Math. Mech.*, **91**(7), 581–593. https://doi.org/10.1002/zamm.201000184.

Liu, S., Yu, T., Bui, T., Yin,, S., Thai, D. and Tanaka, S. (2017), "Analysis of functionally graded plates by a simple locking-free quasi-3D hyperbolic plate isogeometric method", *Comp. Part B: Eng.,* **120**, 182-196. https://doi.org/10.1016/j.compositesb.2017.03.061.

Mohammadi, M., Saidi, A. and Jomehzadeh, E. (2010), "Levy solution for buckling analysis of functionally graded rectangular plates", *Appl. Comp. Mat.*, **17**(2), 81–93. https://doi.org/10.1007/s10443-009-9100-z.

Reddy, J.N. (2000), "Analysis of functionally graded plates", *Int. J. Numer. Methods Eng.*, **47**(1), 663–84. https://doi.org/10.1002/(sici)1097-0207(20000110/30)47:1/3%3C663::aid-nme787%3E3.0.co;2-8.

Soltani, K. Bessaim, A., Houari, M., Kaci, A., Benguediab, M., Tounsi, A. and Alhodaly, M. (2019), "A novel hyperbolic shear deformation theory for the mechanical buckling analysis of advanced composite plates resting on elastic foundations", *Steel Comp. Str*., **30**(1), 13-29. https://doi.org/10.12989/scs.2019.30.1.013.

Swaminathan, K., Naveenkumar, D.T., Zenkour, A.M. and Carrera, E. (2015), "Stress, vibration and buckling analyses of FGM plates – A state-of-the-art review", *Composite Structures*, **120**, 10-31. https://doi.org/10.1016/j.matdes.2006.02.003.

Thai, H.T., Kim, S.E. (2015), "A review of theories for the modeling and analysis of functionally graded plates and shells", *Composite Structures*, **128**, 70-86. https://doi.org/10.1201/9781420092578.ch1.

Valizadeh, N., Natarajan, S., Gonzalez-Estrada, O., Rabczuk, T., Bui, T. and Bordas, S. (2013), "NURBS-based finite element analysis of functionally graded plates: Static bending, vibration, buckling and flutter", *Compos. Str.*, **99**, 309-326. https://doi.org/10.1016/j.compstruct.2012.11.008.

Vu, T., Khosravifard, A., Hematiyan, M. and Bui, T. (2018), "A new refined simple TSDT-based effective meshfree method for analysis of through-thickness FG plates", *Appl. Math. Mod.*, **57**, 514-534. https://doi.org/10.1016/j.apm.2018.01.004.

Yin, S., Hale, J., Yu, T., Bui, T. and Bordas, S. (2014), "Isogeometric locking-free plate element: A simple first order shear deformation theory for functionally graded plates", *Compos. Str.*, **118**, 121-138. https://doi.org/10.1016/j.compstruct.2014.07.028.

Yin, S., Yu, T., Bui, T., Liu, P. and Hirose, S. (2016), "Buckling and vibration extended isogeometric analysis of imperfect graded Reissner-Mindlin plates with internal defects using NURBS and level sets", *Comp. Str.*, **177**, 23-38. https://doi.org/10.1016/j.compstruc.2016.08.005.

Yin, S., Yu, T., Bui, T., Zheng, X. and Tanaka, S. (2016), "In-plane material inhomogeneity of functionally graded plates: A higher-order shear deformation plate isogeometric analysis", *Comp. Part B: Eng.*, **106**, 273-284. https://doi.org/10.1016/j.compositesb.2016.09.008.

Yin, S., Yu, T., Bui, T., Zheng, X. and Yi, G. (2017), "Rotation-free isogeometric analysis of functionally graded thin plates considering in-plane material inhomogeneity", *Thin-Walled Str.*, **119**, 385-395. https://doi.org/10.1016/j.tws.2017.06.033.

Yu, T., Bui, T., Yin, S., Doan, D., Van Do, T., Wu, C. and Tanaka, S. (2016), "On the thermal buckling analysis of functionally graded plates with internal defects using extended isogeometric analysis", *Compos. Str.*, **136**, 684-695. https://doi.org/10.1016/j.compstruct.2015.11.002.

Yu, T., Yin, S., Bui, T., Liu, C. and Wattanasakulpong, N. (2017), "Buckling isogeometric analysis of functionally graded plates under combined thermal and mechanical loads", *Compos. Str.*, **162**, 54-69. https://doi.org/10.1016/j.compstruct.2016.11.084.

*CC*